Available online at www.sciencedirect.com
SCIENCE DIRECT®
PERGAMON
Polyhedron 22 (2003) 1957–1964
POLYHEDRON
www.elsevier.com/locate/poly

Copper(II) complexes with imidazol-4-yl derivatives of 2-imidazoline nitroxides

Elena Fursova [a], Galina Romanenko [b], Vladimir Ikorskii [b], Victor Ovcharenko [b,*]

[a] Novosibirsk State University, Pirogova Str. 2, 630090 Novosibirsk, Russia
[b] International Tomography Center, Russian Academy of Sciences, Institutskaya Str. 3A, 630090 Novosibirsk, Russia

Received 6 October 2002; accepted 16 December 2002

Abstract

$Cu(hfac)_2LH$, $Cu(hfac)_2L^1H$, $Cu(hfac)(CF_3COO)LH$, $Cu(LH)_2(NO_3)_2$, and $Cu(L^1H)_2(NO_3)_2$, where LH and L^1H are nitronyl- and iminonitroxides, respectively, containing an imidazol-4-yl substituent in the side chain have been synthesized. In the solid state, the molecules are linked by intermolecular N–H···O hydrogen bonds, leading to the formation of dimers, bands, or polymer layers. The antiferromagnetic exchange interactions between the odd electrons of the paramagnetic centers are concentrated in the Cu(II)-coordinated nitroxide exchange clusters. The energies of these interactions are between -154 and -350 cm^{-1}.

Keywords: Molecular magnets; Copper(II); Nitroxide; Imidazole; Exchange coupling

1. Introduction

Metal complexes of nitronyl- and iminonitroxides with heterocyclic substituents receive much attention in view of the ability of some of these compounds to undergo cooperative magnetic ordering [1,2] and thermally induced spin transitions [3–6]. This article deals with Cu(II) complexes with spin-labeled imidazol-4-yl derivatives LH and L^1H. Since imidazole derivatives show a clear-cut tendency toward H-bonding in the solid state and in solution [7], it was of interest to trace the type of structure preferably formed by heterospin complexes with LH and L^1H. This study opens the series of our investigations aimed at synthesis, structure analysis, and magnetic studies of metal complexes with various spin-labeled imidazol-4-yl derivatives.

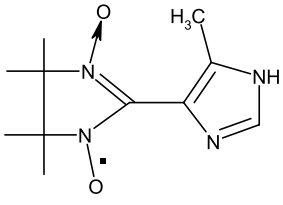

LH

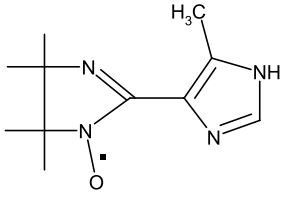

L^1H

2. Experimental

2.1. Synthesis of nitroxides and complexes

2.1.1. 2-(5-Methylimidazol-4-yl)-4,4,5,5-tetramethyl-2-imidazoline-3-oxide-1-oxyl (LH)

Water (50 ml) was poured over a mixture of vicinal bishydroxylamine sulfate monohydrate (12 g) prepared by the procedure of [8,9] and 4-methyl-5-imidazolecarbaldehyde (5 g) (Aldrich, 99%). The mixture was heated

* Corresponding author. Tel.: +7-3832-33-1222; fax: +7-3832-33-1399.
E-mail address: ovchar@tomo.nsc.ru (V. Ovcharenko).

0277-5387/03/$ - see front matter © 2003 Elsevier Science Ltd. All rights reserved.
doi:10.1016/S0277-5387(03)00202-X

to ~50 °C and stirred with a magnetic stirrer for 2 or 3 h. Na_2CO_3 (7 g) was added to the resulting solution in small portions for ~2 h. Vigorous neutralization reaction followed with CO_2 evolution, foaming the reaction mixture. To prevent the foaming, water (~100–150 ml) was added to the reaction mixture simultaneously with Na_2CO_3. The 1,3-dioxyimidazolidine residue was filtered off, washed with water, and dried first in air and then in vacuum at 45 °C for 1 day. This gave 9.3 g of the corresponding 1,3-dioxyimidazolidine. Yield 85%. Found: C 52.4, H 8.3, N 22.0%; Calc. for $C_{11}H_{20}N_4O_2 \cdot 0.75H_2O$: C 52.1, H 8.5, N 22.1%. Then a mixture of 1,3-dioxyimidazolidine (5 g) and PbO_2 (23.5 g) was stirred in $CHCl_3$ (150 ml) at room temperature for 2–3 h. After 30 min, the finely disperse residue of lead oxide precipitated, and the solution was decanted on a paper filter. The residue obtained after the first decanting was treated twice with $CHCl_3$. The consolidated filtrate was centrifuged and passed through a hard-textured filter. The resulting solution of the radical was evaporated to dryness, and the residue was washed with hexane and recrystallized from methanol. After the methanolic solution was stored at −12 °C, LH was obtained as perfect deep violet blue crystals suitable for an X-ray diffraction study. Yield 4 g (80%). Found: C 55.6, H 7.4, N 23.6%; Calc. for $C_{11}H_{17}N_4O_2 \cdot 0.75H_2O$: C 55.6, H 7.2, N 23.6%. M.p. = 183 °C.

2.1.2. 2-(5-Methylimidazol-4-yl)-4,4,5,5-tetramethyl-2-imidazoline-1-oxyl (L^1H)

Water (10 ml) and then $CHCl_3$ (10 ml) was poured over a mixture of LH (0.125 g) and $NaNO_2$ (0.06 g). The dark violet blue two-phase system (LH has good solubility in both water and $CHCl_3$) was stirred for 10 min at room temperature, whereupon ten drops of acetic acid were added, and stirring was continued for 0.5 h. The two-phase system became dark red (L^1H has much better solubility in $CHCl_3$ compared to water). The organic layer was separated and, for more complete extraction of L^1H, the aqueous phase was treated once again with $CHCl_3$ (20 ml) and sodium carbonate (~0.04 g). The consolidated extract was passed through a silica gel column. The product was eluted with a mixture of $CHCl_3$ with ethanol. The eluate was evaporated to dryness. The residue was dissolved in hexane (10 ml). The resulting solution was filtered and stored for 1 day in an open flask at room temperature. After the greater part of hexane evaporated, L^1H formed as red crystals, which were filtered off and dried in air. Yield 0.055 g (45%). Found: C 59.1, H 7.9, N 24.7%; Calc. for $C_{11}H_{17}N_4O$: C 59.7, H 7.7, N 25.3%. M.p. = 143–144 °C.

2.1.3. $Cu(hfac)_2LH$

A mixture of LH (0.05 g) and $Cu(hfac)_2$ (0.1 g) was dissolved in CH_2Cl_2 (15 ml). Then heptane (20 ml) was added. The dark green solution was kept in a loosely closed flask in a dark place at room temperature. After 1 day, violet crystals suitable for an X-ray diffraction study were filtered off. Yield 40%. Found: C 35.9, H 2.7, N 7.3%; Calc. for $Cu(C_5HF_6O_2)_2(C_{11}H_{17}N_4O_2)$: C 35.3, H 2.7, N 7.8%.

2.1.4. $Cu(hfac)_2L^1H$

A mixture of L^1H (0.04 g) and $Cu(hfac)_2$ (0.085 g) was dissolved in CH_2Cl_2 (10 ml). Then heptane (15 ml) was added. The resulting solution was allowed to stay in a loosely stoppered flask in a dark place at room temperature. After 1 day, yellow crystals suitable for an X-ray diffraction analysis were filtered off. Yield 35%. Found: C 36.5, H 2.8, N 7.7%; Calc. for $Cu(C_5HF_6O_2)_2(C_{11}H_{17}N_4O)$: C 36.1, H 2.7, N 8.0%.

2.1.5. $Cu(LH)_2(NO_3)_2$

A solution of $Cu(NO_3)_2 \cdot 3H_2O$ (0.025 mg) in water (4 ml) was carefully poured from a pipet at room temperature to a solution of LH (0.05 g) in water (4 ml). The reaction mixture was stored at room temperature or in a refrigerator. After 15 min, the bulk of the small dark blue crystals of $[Cu(LH)_2](NO_3)_2$ were filtered off. After 1 day, large single crystals suitable for an X-ray diffraction analysis grew in the filtrate. The total yield of the complex was nearly quantitative (~98%). Found: C 39.2, H 5.0, N 20.6%; Calc. for $Cu(C_{11}H_{17}N_4O_2)_2(NO_3)_2$: C 39.9, H 5.2, N 21.2%.

2.1.6. $Cu(L^1H)_2(NO_3)_2$

A solution of $Cu(NO_3)_2 \cdot 3H_2O$ (0.055 mg) in water (2 ml) was poured at room temperature to a solution of L^1H (0.1 g) in water (7 ml). The reaction mixture was stirred and stored in a refrigerator for 2–3 days. The yellow plate-like crystals were filtered off and dried in air. Yield ~20%. Found: C 41.2, H 5.9, N 21.7%; Calc. for $Cu(C_{11}H_{17}N_4O)_2(NO_3)_2$: C 41.9, H 5.4, N 22.2%.

2.2. Magnetic measurements

All measurements were carried out on an MPMS-5S SQUID magnetometer (Quantum Design) in the temperature range of 2–300 K. Molar magnetic susceptibility was calculated using corrections for the diamagnetism of the compounds and temperature independent paramagnetism equal to 60×10^{-6} cm^3 mol^{-1} for Cu(II). The effective magnetic moment was calculated as $\mu_{eff} = (8\chi T)^{1/2}$.

2.3. X-ray crystallography

The data were collected on a Bruker AXS P4 automatic diffractometer at room temperature using the standard procedure (Mo radiation, 0/20 scan mode, variable rate $V_{min} = 3^\circ$ min^{-1} in the range $2 < \theta < 25^\circ$).

Table 1
Crystal data for the compounds and details of experiment

Formula	LH	$Cu(hfac)_2LH$	$Cu(hfac)_2L^1H$	$Cu(hfac)(CF_3COO)LH$	$Cu(LH)_2(NO_3)_2$	$Cu(L^1H)_2(NO_3)_2$
Space group	$P2_1/n$	$P\bar{1}$	$P\bar{1}$	$P2_1/n$	$P2_1/n$	$Pbca$
Unit cell dimensions						
a (Å)	10.010(2)	9.769(2)	9.996(2)	15.782(4)	7.781(2)	6.919(1)
b (Å)	10.021(2)	12.947(3)	12.399(2)	9.350(2)	10.888(2)	30.313(3)
c (Å)	13.092(3)	13.601(3)	13.305(3)	16.971(4)	16.994(3)	14.198(6)
α (°)		99.40(3)	69.01(1)			
β (°)	111.21(3)	110.53(3)	70.28(1)	98.63(2)	101.55(2)	
γ (°)		107.69(3)	72.06(1)			
V (Å^3)	1224.3(4)	1462.9(5)	1416.1(5)	2475.9(10)	1410.4(6)	2978(1)
Z	4	2	2	4	4	8
D_{calc} (g cm^{-3})	1.282	1.623	1.639	1.666	1.559	1.611
μ (mm^{-1})	0.091	0.865	0.889	0.991	0.847	0.817
$I_{h\,k\,l}$ mes/obs	2260/2132	5415/5092	5171/4857	3367/3227	2685/2478	16493/3499
R_{int}	0.0229	0.0396	0.0477	0.0524	0.0486	0.0588
$I_{h\,k\,l}/N$	2132/223	5092/582	4857/546	3227/497	2478/265	3499/243
Goof	1.007	0.899	0.906	0.927	0.796	1.058
R_1 [$I_{h\,k\,l} > 2\sigma(I)$]	0.0385	0.0479	0.0629	0.0617	0.0548	0.0886
wR_2	0.0977	0.0897	0.1124	0.1124	0.1403	0.2452
R_1	0.0556	0.1192	0.1600	0.1726	0.1103	0.1055
wR_2	0.1092	0.1180	0.1487	0.1562	0.1857	0.2595

The structures were solved by direct methods. The full-matrix least-squares refinement was carried out anisotropically for nonhydrogen atoms and isotropically for hydrogen atoms. Some H atoms were localized in difference electron density syntheses, and the others were placed theoretically. All structure solution and refinement calculations were fulfilled using SHELX-97 software. Crystal data for the compounds and details of experiment are listed in Table 1; selected bond lengths and angles are given in Table 2.

3. Results and discussion

3.1. Structure of compounds

An X-ray diffraction study of LH and the complexes confirmed that the N–H protons of the imidazole fragment tend to form hydrogen bonds. Fig. 1 shows the motif of the structure of LH, illustrating the formation of polymer chains based on the N–H···N bonds between the imidazole rings of the neighboring molecules. The distances from the H atom of the imidazole ring to the imine N atom of the imidazole ring and the O atom of the N–O fragment of the neighboring molecule are 2.37 and 2.35 Å, respectively. The angle between the planes of the CN_2 fragment of the imidazoline cycle and the imidazole ring is 38.3°. The N–O bond lengths are virtually the same: 1.279 ± 0.003 Å (Table 2).

The reaction of $Cu(hfac)_2$ with LH in CH_2Cl_2 with subsequent addition of a heptane excess and prolonged storage of the resulting solutions occasionally gave high yields of $Cu(hfac)_2LH$. In most cases, however, after gradual evaporation of CH_2Cl_2 during crystallization of the complex, a dense lacquer-like film of $Cu(hfac)_2LH$ formed under the layer of the mother solution. Sometimes, the film had inclusions of $Cu(hfac)_2LH$ crystals.

Table 2
Selected bond lengths and angles

	LH	$Cu(hfac)_2LH$	$Cu(hfac)(CF_3COO)_2LH$	$Cu(hfac)_2L^1H$	$Cu(LH)_2(NO_3)_2$	$Cu(L^1H)_2(NO_3)_2$
$Cu–O_{NO}$		1.955(3)	1.960(4)		1.975(4)	1.908(4)
$Cu–N_L$				2.018(4)		
$Cu–N_{im}$		1.963(3)	1.951(5)	1.964(3)	1.957(4)	1.945(4)
$Cu–O_{hfac}$		1.947(3)	2.175(5)	1.970(3)	2.556(6)	2.855(5)
		2.295(4)	1.943(4)	1.979(3)		
		2.359(3)	1.965(4)	2.392(4)		
		1.961(3)		2.264(4)		
O–N	1.282(2)	1.297(4)	1.315(5)	1.264(5)	1.316(6)	1.335(5)
	1.277(2)	1.266(5)	1.274(6)		1.273(6)	

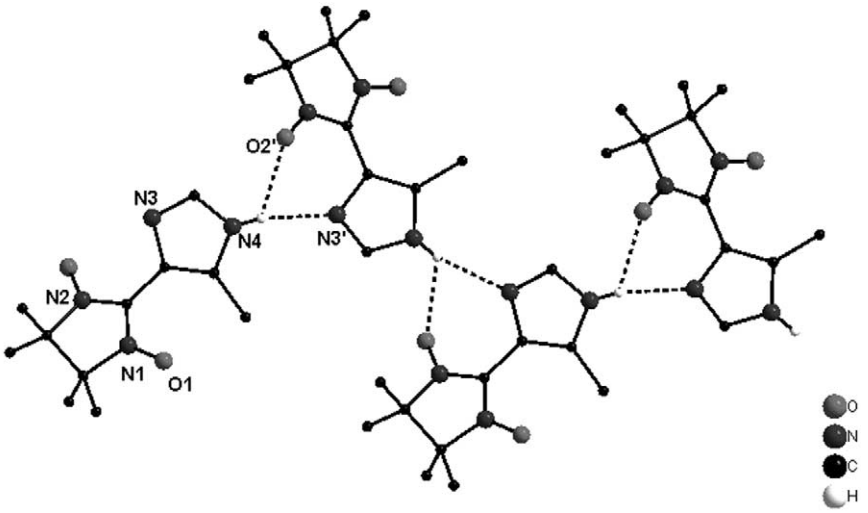

Fig. 1. Chain in the structure of LH (hydrogen atoms omitted for clarity).

Quick removal of CH_2Cl_2 from the CH_2Cl_2/heptane mixture always led to a lacquer-like film not suitable for an X-ray study. The structure of $Cu(hfac)_2LH$ is built of $[Cu(hfac)_2LH]_2$ dimer molecules (Fig. 2(a)) appearing as a result of H-bonding between the N–H group of the imidazole ring of one of the $\{Cu(hfac)_2LH\}$ fragments and the O atom of the hfac-anion of the neighboring $\{Cu(hfac)_2LH\}$ fragment. In each $\{Cu(hfac)_2LH\}$ fragment, the copper atom is surrounded by a square bipyramid, whose base is formed from the donor atoms of the paramagnetic ligand ($Cu–O_{LH}$ 1.95 and $Cu–N_{LH}$ 1.96 Å) and one O atom from each of the two hfac-anions ($Cu–O_{hfac}$ 1.95–1.96 Å); the other two O_{hfac} atoms occupy the axial positions (Cu–O 2.29–2.36 Å). Thus the paramagnetic LH in the $\{Cu(hfac)_2LH\}$ fragments is coordinated as a bidentate ligand, and the H-bonds inside the binuclear $[Cu(hfac)_2LH]_2$ molecule are formed by the imidazole N–H groups lying on the 'periphery' of the $\{Cu(hfac)_2LH\}$ fragment. Thus even when complexed, LH still tends to form H-bonds. Dimerization at the expense of two $N–H\cdots O_{hfac}$ bonds forming $[Cu(hfac)_2LH]_2$ with the dimer molecules surrounded by the CH_3 and CF_3 groups in the 'outer sphere' is possibly responsible for the formation of perfect crystals of the complex from nonpolar heptane. If, however, some other factors (not stated here) hinder the formation of such symmetric binuclear molecules, the solid phase is an amorphous glassy film. No such films have even been recorded during crystallization of $Cu(hfac)_2L^1H$, whose structure is formed from the same binuclear molecules as in the case of $Cu(hfac)_2LH$ (Fig. 2(b), Table 2). The only difference between $[Cu(hfac)_2LH]_2$ and $[Cu(hfac)_2L^1H]_2$ lies in the 5-membered chelate ring formed by the paramagnetic ligand and the metal in the case of $[Cu(hfac)_2L^1H]_2$.

In solution, LH and L^1H are also kinetically stable. For reasons stated below, the filtrates remaining after the isolation of $Cu(hfac)_2LH$ crystals or the mother solutions together with the lacquer film were stored for prolonged times under normal conditions (from a few days to several weeks). No products of LH decomposition have ever been recorded in this case. On the contrary, after many weeks of storage of the mother solution and separation of $Cu(hfac)_2LH$ crystals and

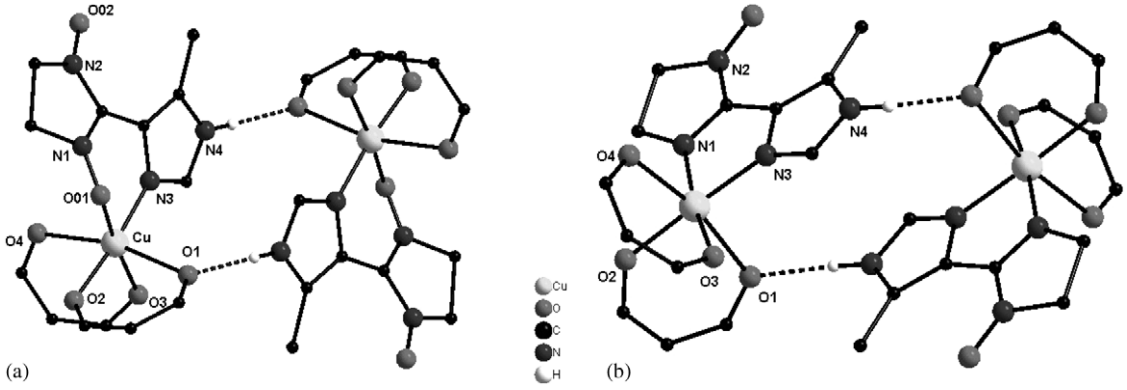

Fig. 2. Structure of binuclear $[Cu(hfac)_2LH]_2$ (a) and $[Cu(hfac)_2L^1H]_2$ (b) molecules (CH_3 and CF_3 groups omitted for clarity).

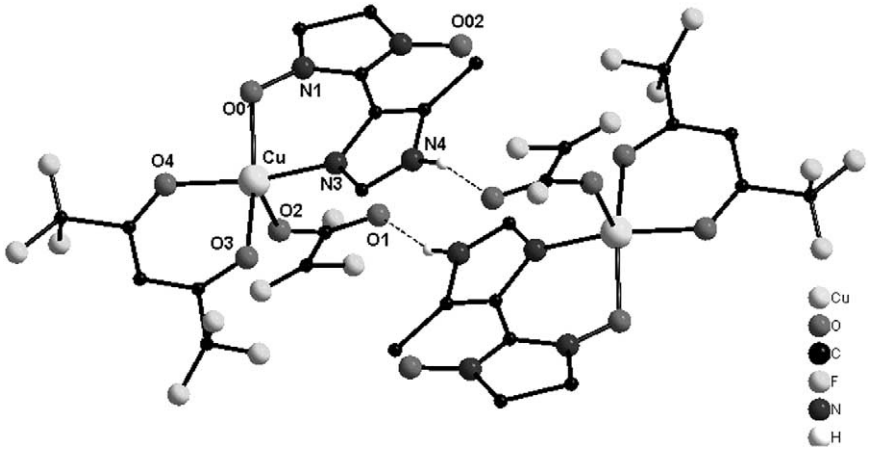

Fig. 3. Structure of the dimer in Cu(hfac)(CF_3COO)HL (CH_3 groups and hydrogen atoms omitted for clarity).

then of the lacquer film (i.e. after removal of the bulk product), a few light yellow crystals formed. A synthetic procedure has not been worked out specially for this product; here we restrict ourselves to a brief description of the structure of the crystals formed from the binuclear [Cu(hfac)(CF_3COO)LH]$_2$ molecules (Fig. 3). This complex contains not only the hfac-anion, but also the product of its hydrolysis—CF_3COO-anion. As a result of a great number of lengthy manipulations with the solution of reagents (Cu(hfac)$_2$+LH), hfac was partially destroyed in the CH_2Cl_2/heptane mixture, whereas the paramagnetic ligand remained intact. In [Cu(hfac)(CF_3COO)LH]$_2$ molecules (Fig. 3), the coordination number of each Cu atom is 5. The square pyramidal environment of Cu is formed from two O atoms of the hfac-anion, the N–O oxygen atom, and the imine N atom of the imidazole ring of LH (Cu–O_{hfac} 1.94 and 1.96, Cu–O_{LH} 1.96, Cu–N_{LH} 1.95 Å) lying at the base of the pyramid. The apex of the pyramid is formed by one of the O atoms of the trifluoroacetate anion (Cu–O_{CF_3COO} 2.17 Å). The other atom is involved in the O···H–N H-bond with the imidazole ring of the neighboring {Cu(hfac)(CF_3COO)LH} fragment (O···N 2.705 Å). Thus in the structure of Cu(hfac)(CF_3-COO)LH, the paramagnetic ligand also demonstrates a tendency toward formation of H-bonds, linking the {Cu(hfac)(CF_3COO)LH} fragments into dimers.

With all the difficulties in crystal growth of heterospin complexes of Cu(hfac)$_2$ with LH and L^1H, the complexes were isolated and their structure was determined. Crystals of analogous complexes based on M(hfac)$_2$, where M = Ni, Co, Mn, were not grown, since concentration of their solutions led to viscous resins which solidified into glassy mass. Therefore we attempted to grow ionic complexes with LH from water, i.e., in conditions of the complete absence of an organic solvent from the mother solution. We failed to obtain heterospin crystals suitable for an X-ray study from aqueous solutions of Ni(II) or Co(II) salts with LH or L^1H. Note that in our experiments the reaction of $Ni(NO_3)_2 \cdot 6H_2O$ with LH in water always produced perfect 'single crystals', which gave no diffraction reflections.

Perfect crystals were obtained by carefully mixing an aqueous solution of Cu(II) nitrate with an aqueous solution of LH or L^1H. This procedure formed $Cu(LH)_2(NO_3)_2$ or $Cu(L^1H)_2(NO_3)_2$ crystals, respectively, suitable for a structural study. Fig. 4 shows a fragment of the structure of $Cu(LH)_2(NO_3)_2$ projected on the (0 1 0) plane. The centrosymmetric square environment of each copper atom formed by the O

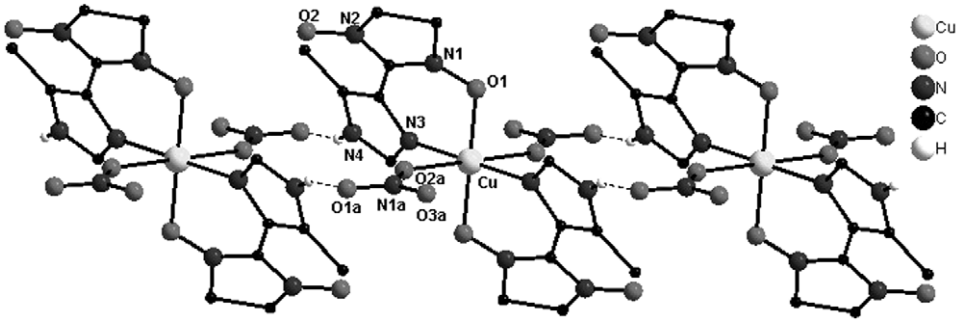

Fig. 4. Formation of ribbons in the structure of $Cu(LH)_2(NO_3)_2$ (CH_3 groups and hydrogen atoms omitted for clarity).

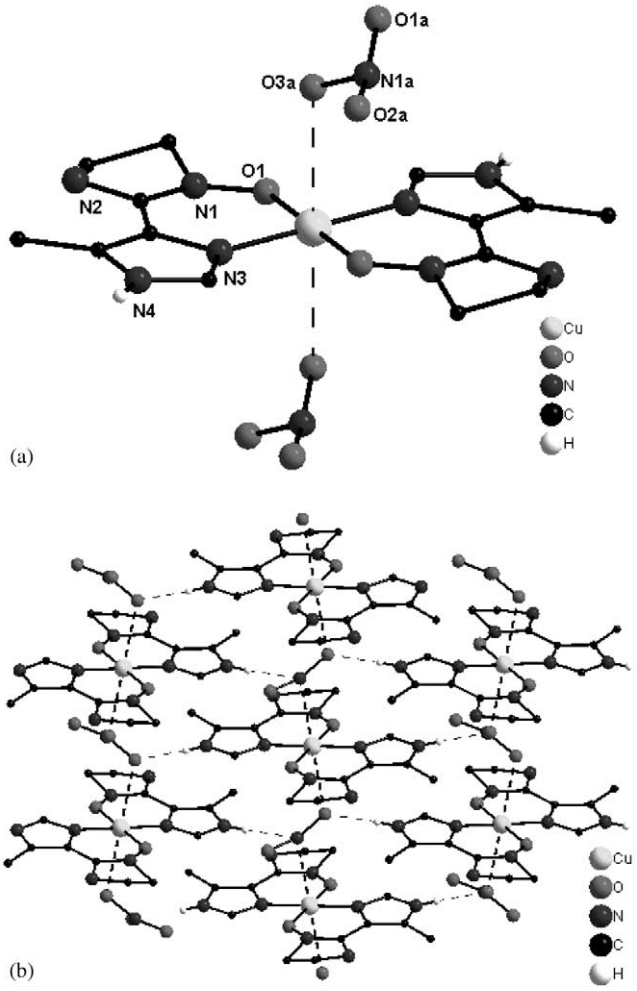

Fig. 5. Environment of the copper atom (a) and scheme of layer formation in $Cu(L^1H)_2(NO_3)_2$ (b) (CH_3 groups and hydrogen atoms omitted for clarity).

atoms of the N–O group of the imidazoline cycle and the imine N atoms of the imidazole ring of the two bidentate ligands LH ($Cu–O_{LH}$ 1.97, $Cu–N_{LH}$ 1.95 Å) is completed to octahedral by the O atoms of the two NO_3^- groups ($Cu–O_{NO_3}$ 2.55 Å). All N–H groups of the imidazole rings are linked by H-bonds with the nitrate anions, leading to formation of ribbons in solid $Cu(LH)_2(NO_3)_2$ (Fig. 4).

In the structure of $Cu(L^1H)_2(NO_3)_2$ (Fig. 5) as well as in $Cu(LH)_2(NO_3)_2$, the centrosymmetric square environment of each Cu atom is formed from the O atoms of the N–O group of the imidazoline cycle and the imine N atoms of the imidazole ring of the two bidentate ligands L^1H ($Cu–O_{L^1H}$ 1.91, $Cu–N_{L^1H}$ 1.94 Å). In contrast to $Cu(LH)_2(NO_3)_2$, the square environment is not completed to octahedral, because the $Cu–O_{NO_3}$ short contacts are at least 2.85 Å (Table 2). If, however, these contacts as well as the hydrogen bonds between the N–H fragments of the imidazole rings and the oxygen atoms of the NO_3-anions (N···O 2.75–2.86 Å) (dashed lines in Fig. 5) are taken into consideration, then the structure of $Cu(L^1H)_2(NO_3)_2$ may formally be regarded as layered polymer. Summing up the discussion of the structures of the Cu(II) complexes with LH and L^1H under study, we note that in the complex with LH the angle between the planes of the CN_2 fragment of the imidazoline cycle and the imidazole ring does not change and equals 25.1–28.8°. In $Cu(L^1H)_2(NO_3)_2$, this angle is considerably smaller (0.9°) because there is no steric hindrance to the coplanar arrangement of heterocycles in the molecule.

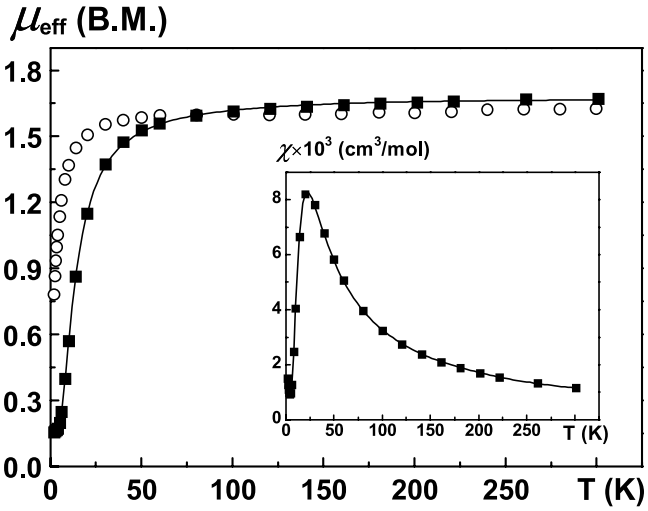

Fig. 6. Temperature dependences of μ_{eff} for the radicals LH (■) and L^1H (○). Insert-curve $\chi(T)$ for LH.

3.2. Magnetic properties

Fig. 6 shows the dependences $\mu_{eff}(T)$ for LH and L^1H. Magnetic susceptibility and μ_{eff} for L^1H have no anomalies and obey the Curie–Weiss law ($C = 0.35$ cm^3 K mol^{-1}, $\theta = -4.0$ K). The curve $\chi(T)$ for LH has a maximum at 23 K (Fig. 6, insert). Above the temperature of the maximum, magnetic susceptibility also follows the Curie–Weiss law with the parameters $C = 0.37$ cm^3 K mol^{-1} and $\theta = -11.7$ K. For both radicals, the values of C are close to the theoretical value of 0.375 cm^3 K mol^{-1} for an odd electron.

The dependence $\chi(T)$ for LH is well approximated by the Bleaney–Bowers model:

$$\chi_{dim} = \frac{N\beta^2 g^2}{3kT}\left[1 + \frac{1}{3}\exp\left(\frac{-2J}{kT}\right)\right]^{-1}$$

where J is the exchange parameter ($H = -2JS_1S_2$); the g-factor of LH was taken to be 2. The optimization procedure gave $J = -12.4$ cm^{-1} for the minimal sum of square deviations $\sigma = \Sigma_{i=1}^{n}[\mu_{eff}^{ex}(T_i) - \mu_{eff}^{calc}(T_i)]^2 = 5.9 \times 10^{-4}$. For L^1H, the exchange parameter was evaluated in the framework of the molecular field approximation [10] using the expression relating the exchange para-

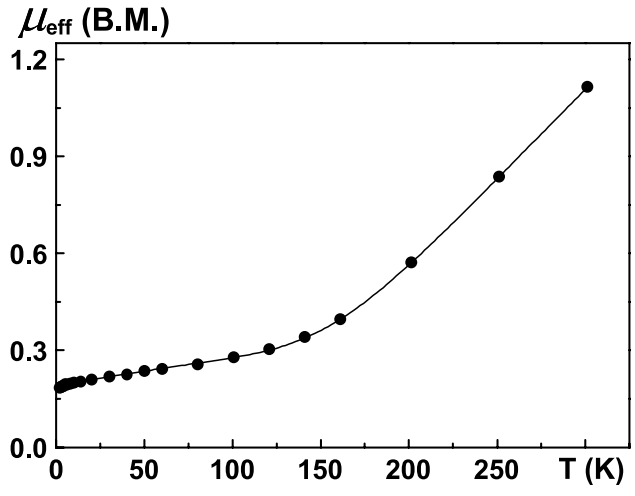

Fig. 7. Dependence $\mu_{eff}(T)$ for $Cu(hfac)_2LH$.

meter with the Weiss constant: $\theta = 2nJS(S+1)/3k$. As a result, it was obtained that $nJ = -5.6$ cm^{-1}. Thus, in solid LH and L^1H, antiferromagnetic intermolecular exchange interactions take place.

In $Cu(hfac)_2LH$, the antiferromagnetic exchange interactions are concentrated in quasiisolated intramolecular exchange clusters Cu(II)–O$^\bullet$–N<, where the Cu(II)–O distances equal to 1.95 Å. At lower temperatures, the value of μ_{eff} of the complex (Fig. 7) decreases drastically, tending to the limit ~ 0.19 B.M. The presence of this residual moment at low temperatures may be attributed to the $\sim 1.2\%$ monomer admixture in the form of $Cu(hfac)_2$ or LH. Taking into account this admixture, we described (Fig. 7) the experimental dependence $\mu_{eff}(T)$ in terms of the model of the heterospin exchange cluster Cu(II)–O$^\bullet$–N< [11]. To calculate the energy levels of the cluster in the external magnetic field we employed the isotropic spin Hamiltonian

$$\hat{H} = -2J\hat{s}\hat{s}_L - \beta(g\hat{s}zg_L\hat{s}_L^z)H - 2nJ'\hat{S}_z\langle\hat{S}_z\rangle$$

where J and nJ' are the intra and interclaster exchange parameters, $\hat{s}$ and $\hat{s}_L$ and are the spin operators of Cu(II) and nitroxide, $\hat{S} = \hat{s} + \hat{s}_L$ is the total spin operator of the cluster, g and g_L are the g factors of Cu(II) and nitroxide, n is the number of the nearest-neighbor molecules, β the Bohr magneton, and $\langle\hat{S}_z\rangle$ is its averaged projection onto the z axis. Processing of experimental data for $Cu(hfac)_2LH$ gave the following optimal parameters of the spin Hamiltonian: $g = 2.1$, $g' = 2$, $J = -360$ cm^{-1}, $nJ' = -0.8 \times 10^{-3}$ cm^{-1}, $\sigma = 1.2 \times 10^{-3}$.

In the structures of $Cu(LH)_2(NO_3)_2$ and $Cu(L^1H)_2(NO_3)_2$, one can also distinguish quasiisolated exchange clusters >N–$^\bullet$O–Cu(II)–O$^\bullet$–N< with direct exchange. The dependence $\mu_{eff}(T)$ for $Cu(LH)_2(NO_3)_2$ is approximated by the three-center heterospin exchange cluster with an isotropic spin Hamiltonian [11]:

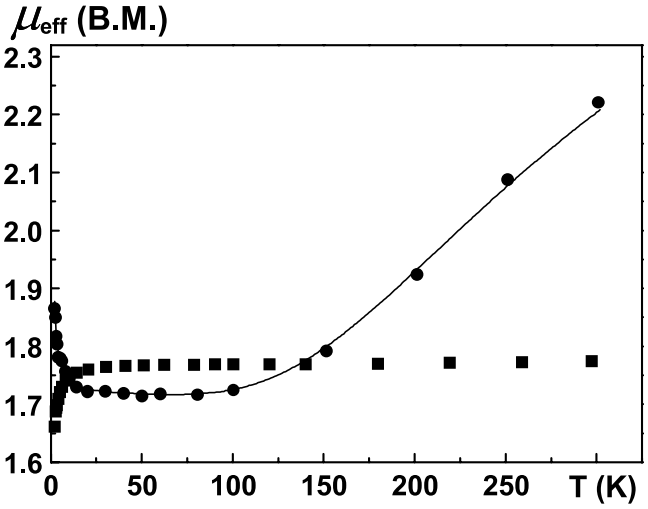

Fig. 8. Temperature dependences of μ_{eff} for $Cu(L^1H)_2(NO_3)_2$ (■) and $Cu(LH)_2(NO_3)_2$ (●).

$$\hat{H} = -2J\hat{s}\hat{s}' - \beta(gs_z + g's'_z)H - 2nJ'\hat{S}_z\langle\hat{S}_z\rangle$$

where J and nJ' are the intra and intercluster exchange parameters, $\hat{s}$ is the spin operator of Cu(II), $\hat{s}' = \hat{s}_1 + \hat{s}_2$ is the total spin operator of two radicals, g and g' are the g factors of Cu(II) and nitroxide, n is the number of nearest-neighbor molecules, $\hat{S} = \hat{s} + \hat{s}'$ is the total spin operator of the cluster, and $\langle\hat{S}_z\rangle$ is its averaged projection onto the z axis. The optimal J, nJ', and g_{Cu} ($g_L \equiv 2$) values for $Cu(LH)_2(NO_3)_2$ are: $g_{Cu} = 2.06$, $J = -154$ cm^{-1}, $nJ' = 0.5$ cm^{-1}, $\sigma = 2.3 \times 10^{-4}$. Note that at low temperatures, the exchange interactions of uncompensated spins $S = 1/2$ in $Cu(LH)_2(NO_3)_2$ are ferromagnetic, as indicated by the sign of the nJ' parameter and increased μ_{eff} below 20 K (Fig. 8).

The value of μ_{eff} for $Cu(L^1H)_2(NO_3)_2$ (Fig. 8) is virtually constant above 20 K; it corresponds to one odd electron per complex molecule. This is a consequence of stronger ($> |500|$ cm^{-1}) intracluster exchange interactions compared to $Cu(LH)_2(NO_3)_2$. In the region below 20 K, μ_{eff} decreases with temperature, indicating that the exchange interactions between the residual spins $S = 1/2$ are antiferromagnetic. The stronger antiferromagnetic character of the exchange interactions in $Cu(L^1H)_2(NO_3)_2$ compared to $Cu(LH)_2(NO_3)_2$ may be attributed to the shorter Cu–O distances (Table 2) in the >N–$^\bullet$O–Cu(II)–O$^\bullet$–N< exchange clusters in solid $Cu(L^1H)_2(NO_3)_2$.

4. Supplementary material

Crystal data for the structural analysis for LH, $Cu(hfac)_2LH$, $Cu(hfac)_2L^1H$, $Cu(hfac)(CF_3COO)LH$, $Cu(LH)_2(NO_3)_2$, $Cu(L^1H)_2(NO_3)_2$ have been deposited with the Cambridge Crystallographic Data Centre, CCDC Nos. 199132–199137. Copies of this information

may be obtained free of charge from the Director, CCDC, 12 Union Road, Cambridge, CB21EZ, UK.

Acknowledgements

Research funded in part by US Civilian and Development Foundation (grant REC-008), RFBR (grants 00-03-32518, 02-03-33112), Minobr RF (grant E-02 5.0-188) and Integration program 146.

References

[1] K. Fegy, D. Luneau, E. Belorizky, M. Novac, J.-L. Tholence, C. Paulsen, T. Ohm, P. Rey, Inorg. Chem. 37 (1998) 4524.
[2] K. Fegy, D. Luneau, T. Ohm, C. Paulsen, P. Rey, Angew. Chem., Int. Ed. 37 (1998) 1270.
[3] F. Lanfranc de Panthou, E. Belorizky, R. Calemczuk, D. Luneau, C. Marcenat, E. Ressouche, P. Turek, P. Rey, J. Am. Chem. Soc. 37 (1995) 11247.
[4] F. Lanfranc de Panthou, D. Luneau, R. Musin, L. Ohrstrom, A. Grand, P. Turek, P. Rey, Inorg. Chem. 35 (1996) 3484.
[5] V.I. Ovcharenko, S.V. Fokin, G.V. Romanenko, V.N. Ikorskii, E.V. Tretyakov, S.F. Vasilevsky, J. Struct. Chem. 43 (2002) 153.
[6] V.I. Ovcharenko, S.V. Fokin, G.V. Romanenko, V.N. Ikorskii, E.V. Tretyakov, S.F. Vasilevsky, R.Z. Sagdeev, Mol. Phys. 100 (2002) 1107.
[7] T.L. Gilchrist, Heterocyclic Chemistry, second ed., Longman Scientific & Technical, London, 1992.
[8] V. Ovcharenko, S. Fokin, P. Rey, Mol. Cryst. Liq. Cryst. 334 (1999) 109.
[9] V.I. Ovcharenko, S.V. Fokin, G.V. Romanenko, I.V. Korobkov, P. Rey, Russ. Chem. Bull. 48 (1999) 1519.
[10] S. Smart, Effective Field Theories of Magnetism, W.B. Saunders Company, Philadelphia, London, 1966, p. 271.
[11] I.V. Ovcharenko, Y.G. Shvedenkov, R.N. Musin, V.N. Ikorskii, J. Struct. Chem. 40 (1999) 29.